Experimental determination of exchange constants in antiferromagnetic Mn_2Au

A.A. Sapozhnik,[1,2] C. Luo,[3,4] H. Ryll,[3] F. Radu,[3]
M. Jourdan,[1,2] H. Zabel,[1,2] and H.-J. Elmers[1,2]

[1] *Institut für Physik, JGU Mainz, Staudingerweg 7, 55128, Mainz, Germany*

[2] *Graduate School Materials Science in Mainz, Staudingerweg 9, 55128, Mainz, Germany*

[3] *Helmholtz-Zentrum Berlin für Materialien und Energie, Albert-Einstein Str. 15, 12489, Berlin, Germany*

[4] *Institut für Experimentelle und Angewandte Physik, Universität Regensburg, Universitätsstrasse 31, 93053 Regensburg, Germany*

Abstract

Mn_2Au is an important antiferromagnetic (AF) material for spintronics applications. Due to its very high Néel temperature of about 1500 K, some of the basic properties are difficult to explore, such as the AF susceptibility and the exchange constants. Experimental determination of these parameters is further hampered in thin films by unavoidable presence of uncompensated and quasi-loose spins on antisites and at interfaces. Using x-ray magnetic circular dichroism (XMCD), we have measured induced perpendicular spin and orbital moments for a $Mn_2Au(001)$ film in fields up to ± 8 T. By performing these measurements at a low temperature of 7 K and at room temperature (RT), we were able to separate the loose spin contribution from the susceptibility of AF coupled spins. The value of the AF exchange constant obtained with this method for a 10 nm thick $Mn_2Au(001)$ film is (22 ± 5) meV.

I. INTRODUCTION

At present, antiferromagnets (AF) play an important role in the rapidly growing field of AF spintronics [1] due to their fast THz dynamics [2–5]. In the past, AF materials have been exploited for providing exchange bias in spin valves [6]. However, at present AF materials are in the focus of interest for their own right, for instance, for magnetization switching by (unpolarized) electrical currents, proposed for designing the next generation data storage devices [7, 8]. One of the main requirements for prospective AF applications is the magnetic order stability at RT. The characteristic temperature up to which the material preserves its magnetic order is called Néel temperature (T_{N}). The majority of the antiferromagnetic materials have T_{N} either lower or close to RT [1]. Only a few metallic AFs exist, which are suitable for spintronics application above RT, including Mn_2Au with a very high T_{N} of 1500 K in a bulk crystal [9].

According to quantum statistics considerations, T_{N} depends on the exchange interaction strength in a material, which defines the mean effective Weiss field stabilizing the antiparallel spin alignment. The exchange interaction between two spin moments i^{th} and j^{th} can be described in terms of exchange constants J_{ij} depending on the distance between the corresponding atoms [10]. Another characteristic of non-perfect AF compounds is the existence of weakly coupled and loose paramagnetic spins at antisite defects, at interfaces, and, in addition, at grain boundaries in polycrystalline and epitaxial thin films.

The exchange constants J_{ij} of antiferromagnets can be determined from the perpendicular susceptibility, i.e. the spin response to a magnetic field applied perpendicular to the AF spins. The standard tools for measuring the perpendicular susceptibility are either magnetometry or neutron scattering. In contrast to the mentioned methods, x-ray magnetic circular dichroism (XMCD) provides element specific data about the magnetic properties of the investigated material and is sensitive to several nanometers at the surface in the total electron yield (TEY) mode. Owing to the sum rules [11, 12], XMCD allows accessing the spin and orbital magnetic moment values separately, leading to further insight into the magnetic properties of AFs.

In this contribution, we report on experimental results for the perpendicular magnetic susceptibility in the ordered AF phase of Mn_2Au using XMCD. The results obtained at 7 K and at RT allow to distinguish contributions from uncoupled (loose) spins with paramagnetic

behavior and AF coupled spins with a small and constant perpendicular susceptibility. From the response of AF coupled spins we obtain an experimental value for the exchange constant. In addition, the determined ratio of the measured orbital and spin moments sheds light on the coupling mechanism of magnetic moments in antiferromagnetic compounds.

II. METHODS

Mn_2Au epitaxial thin films were deposited by radio frequency magnetron sputtering on a $Al_2O_3(1\bar{1}02)$ substrates. The base pressure in the sputtering chamber was $\sim 10^{-8}$ mbar. The prepared sample has the following layer structure Al_2O_3/ Ta(001) 15 nm/ Mn_2Au(001) 10 nm/ AlO_x 2 nm. The Ta buffer ensures the necessary (001) orientation of Mn_2Au. The film surface was coated with an Al capping layer for oxidation protection. The sample structure was characterized with x-ray diffraction (XRD) and reflection high-energy electron diffraction (RHEED) to prove its high surface and bulk quality [13]. The average grain size in the Mn_2Au film estimated from the XRD spectrum using the Scherrer equation is 15 nm in the sample plane. A stoichiometry of $(66.2 \pm 0.3)\,\%$ Mn and $(33.8 \pm 0.3)\,\%$ Au was determined by energy-dispersive x-ray spectroscopy (EDX) indicating a slight Au excess. Details about the preparation and characterization procedures are reported in [13].

The XMCD spectroscopy measurements were performed with the VEKMAG end station [14] at BESSY II, Helmholtz-Zentrum Berlin (HZB), Germany, during the multi-bunch operational mode of the synchrotron storage ring. The sample was placed in the chamber at a pressure of $\sim 2 \times 10^{-10}$ mbar in the gap of a superconducting magnet. The x-ray absorption spectra (XAS) were measured for x-ray energies in the vicinity of the L_3 and L_2 absorption edges of Mn. The photocurrent was normalized to the current of a Pt-mesh monitor located in the x-ray beam path in order to compensate for variations of the ring current and for the transmission function of the optical elements. The XMCD spectrum was obtained as the difference of XAS measured for circular right and left x-ray polarizations with a polarization degree of 77 %.

The Mn_2Au density of states (DOS) was calculated with the FP-LAPW ELK software [15]. The lattice constants were set equal to the published values of $a = 3.328$ Å and $c = 8.539$ Å [16]. The staggered magnetization direction orientation was chosen to be along the $\langle 110 \rangle$ crystallographic directions [17]. The spin-orbit coupling is self-consistently added to

the second-variational Hamiltonian. A set of 1728 k-points distributed over the first Brillouin zone was used in the numeric scheme. The total energy error was less than 0.1 meV/f.u..

III. THEORETICAL RESULTS

It was demonstrated by Barthem et al. [9] that Mn_2Au has a layered antiferromagnetic structure with two sublattices denoted as Mn I and Mn II. The calculated Mn_2Au DOS indicates that the Mn atoms carry a magnetic moment [Fig. 1], whereas the Au atoms do not feature a magnetic moment, confirmed by the identical DOS for majority and minority electrons. The DOS of Mn II atoms (not shown) is found to be opposite to the DOS of Mn I atoms.

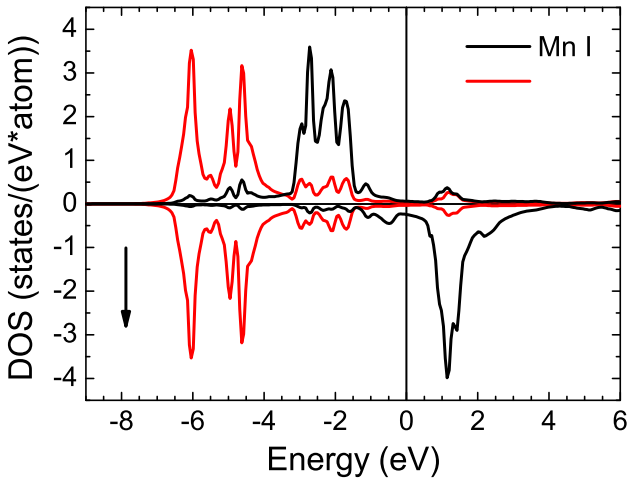

FIG. 1. Element resolved DOS of Mn_2Au. Positive and negative DOS values correspond to spin-up (majority) and spin-down (minority) electrons, respectively.

The simulation provides the following Mn spin moment $\mu_{\mathrm{S}}^{\mathrm{Mn}} = \pm 3.591\,\mu_B$ and orbital moment $\mu_{\mathrm{L}}^{\mathrm{Mn}} = \mp 0.002\,\mu_B$. The value of $\mu_{\mathrm{L}}^{\mathrm{Mn}}$ is much smaller than $\mu_{\mathrm{S}}^{\mathrm{Mn}}$, which is typical for transition metal elements due to orbital moment quenching [18]. Another important property of Mn_2Au obtained from the DOS is the number of d-holes per Mn atom $N_m athrmd$, which amounts to 5.0.

In the following, we discuss expected contributions to the field-induced magnetic moments based on the calculated total magnetic moments. In general, the perpendicular magneti-

zation induced in Mn_2Au by an external field contains two contributions. One of them is generated by the rotation of the exchange coupled moments. Due to the high T_N of Mn_2Au, thermal excitations can be neglected below RT. Thus, the coupled moment contribution is expected to be linearly proportional to the applied field. The ratio of the resulting magnetic moment in the direction perpendicular to the film and the applied magnetic field value then provides the perpendicular susceptibility $\chi_\perp = M_\perp/(\mu_0 H)$. In the case of Mn_2Au, the induced magnetic moment is expected to be very small. The order of magnitude of the induced moment can be estimated from the susceptibility $\chi = 5 \times 10^{-4}$ measured in Ref. [9]. Using the saturation magnetization of Mn_2Au $M_S = 1.56 \times 10^6\,\mathrm{A\,m^{-1}}$ results in $M_\perp/M_S = 0.2\,\%$ at 8 T. However, the powder samples investigated in Ref. [9] represent an average over randomly oriented bulk crystallites.

The second contribution originates from uncoupled (loose) Mn moments. Absence of exchange coupling implies that the induced magnetization can be described by the Brillouin function:

$$\frac{M^{\mathrm{loose}}}{M_S^{\mathrm{loose}}} = B_J\left(\frac{g\mu_B J \mu_0 H}{k_B T}\right), \tag{1}$$

where M^{loose} and M_S^{loose} are the induced perpendicular magnetization and saturation magnetizations of the loose spins, respectively, and g is the gyromagnetic ratio. Since μ_L^{Mn} is much smaller than μ_S^{Mn}, J is replaced by $S = 1.8$ in the following discussion. M_S^{loose} depends on the concentration of the uncoupled spins, the value of which is to be determined from the experiment. However, in epitaxial magnetic films their concentration is expected to be rather small. This assumption is scrutinized for our samples in Section V. Substituting the experimental values of $\mu_0 H = 8\,\mathrm{T}$ and $T = 300\,\mathrm{K}$ into Eq. (1) results in $M^{\mathrm{loose}} = 0.03\,M_S^{\mathrm{loose}}$. Thus, the induced magnetization of loose spins at RT amounts to only 3 % of its saturation value and can be neglected. As a consequence, the induced perpendicular magnetization at RT is solely due to the antiferromagnetically coupled spins. This implies that the exchange constant of AF Mn_2Au thin films can be determined at RT by measuring the induced magnetic moment at the highest available external field. According to Eq. (1), $M^{\mathrm{loose}} = 0.74\,M_S^{\mathrm{loose}}$ at a temperature of 7 K. Thus, at low temperatures the contribution of the loose spins is expected to be more significant and to constitute a substantial part of the measured magnetic signal.

IV. EXPERIMENTAL RESULTS

The x-ray absorption spectra (XAS) were measured for right and left circular x-ray polarization in a field of 8 T applied to the sample at 300 K [Fig. 2(a)] and at 7 K [Fig. 2(b)]. The XMCD spectra resulting from the difference of two XAS at the respective temperatures are shown in Figs. 2(c) and 2(d).

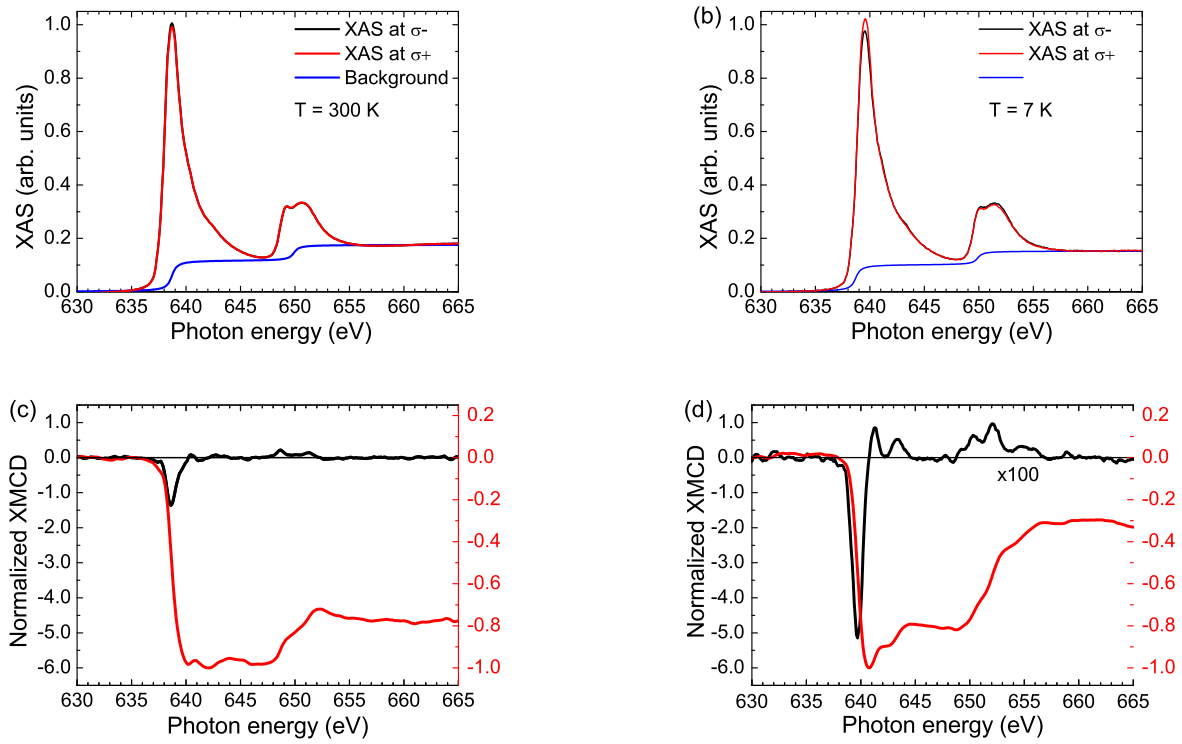

FIG. 2. XAS measured for the Mn_2Au film at 300 K (a) and 7 K (b), respectively, while applying 8 T out-of-plane magnetic field corresponding to circular positive (black) and negative (red) polarization. The blue line shows the contribution of the delocalized electrons to x-ray absorption. (c, d) XMCD calculated with the data presented in (a) and (b), respectively. The XMCD values are the difference between the corresponding XAS spectra multiplied by 100.

The sum rules [11, 12] were employed for determining the values of spin and orbital

momentsin the following form:

$$
\begin{aligned}
A &= \int_{L_3} XMCD(E)\, dE, \\
B &= \int_{L_2} XMCD(E)\, dE, \\
C &= \int_{L_3+L_2} \frac{XAS_{\sigma+}(E) + XAS_{\sigma-}(E)}{2}\, dE, \\
\mu_L &= -N_d \frac{Corr_{jj}}{P} \frac{2(A+B)}{3C} \mu_B, \\
\mu_S &= -N_d \frac{Corr_{jj}}{P} \frac{A-2B}{C} \mu_B,
\end{aligned}
\tag{2}
$$

where N_{d} is the number of 3d holes in Mn, $Corr_{jj} = 1.4$ is the correction factor compensating for the jj-mixing [19, 20], $P = 0.77$ is the degree of circular polarization provided by the beamline.

a. High temperature measurements

For the spectra measured at RT, integrals in Eq. (2) result in $A = -1.68 \pm 0.11$, $B = 0.33 \pm 0.03$, and $C = 3.17 \pm 0.09$ [Fig. 2(c)]. The obtained spin and orbital moments are $\mu_S = (0.065 \pm 0.010)\,\mu_{\mathrm{B}}$ and $\mu_{\mathrm{L}} = (0.025 \pm 0.005)\,\mu_{\mathrm{B}}$. The corresponding rotation angle of the spin moment towards the film normal is $\approx 1^{\circ}$. The experimentally determined orbital moment is much larger than the theoretical value $\mu_{\mathrm{L}}^{\mathrm{Mn}}$ presented in the Section III and amounts to about 30 % of μ_{S}. We recall that, as discussed in Section III, the high temperature results are mainly due to the antiferromagnetically coupled Mn moments in the AF films and not due to the loose spins.

b. Low temperature measurements

At low temperatures, we observe a considerably larger value of XMCD [Fig. 2(b)]. For these spectra, we calculate $A = -4.91 \pm 0.36$, $B = 2.91 \pm 0.08$, $C = 3.35 \pm 0.07$ [Fig. 2(d)]. This yields $\mu_S = (0.27 \pm 0.04)\,\mu_{\mathrm{B}}$/atom and $\mu_L = (0.048 \pm 0.015)\,\mu_{\mathrm{B}}$/atom. The field dependence of the spin and orbital moments is shown in Fig. 3.

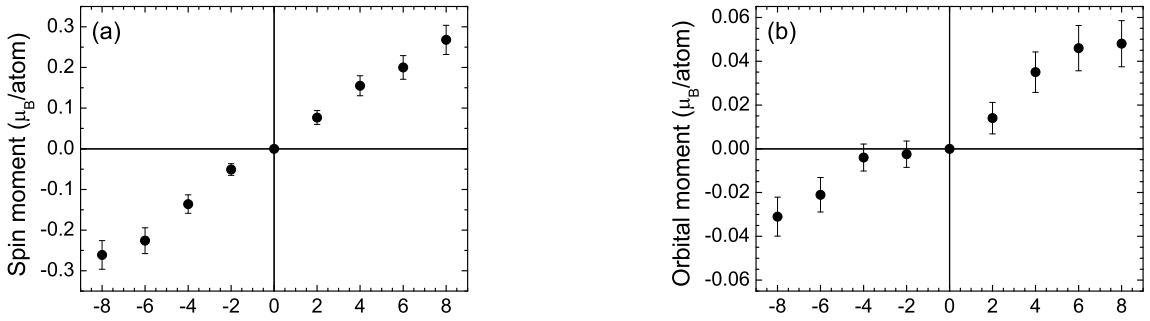

FIG. 3. (a) Field dependence of induced perpendicular spin magnetic moment per Mn atom at a temperature of 7 K calculated from the corresponding XMCD spectra with sum rules. (b) The same for orbital magnetic moment.

V. DISCUSSION

a. Perpendicular susceptibility of AF coupled spins

The model used for describing the perpendicular susceptibility of Mn_2Au employs three exchange constants, which describe the antiferromagnetic interaction between the neighboring Mn planes in Mn_2Au (J_1 and J_2) and the ferromagnetic interaction within one layer of Mn atoms (J_3) [Fig. 4]. An external field applied along the [001] axis tilts the Mn moments such that the parallel alignment within the basal *ab*-planes is preserved. Therefore, the exchange energy gain does not depend on J_3. A Mn atom is coupled to the four nearest neighbors with strength J_1 and to the next nearest neighbor across the layer of Au atoms with strength J_2. This corresponds to the effective constant $J_{\rm eff} = (4\,J_1 + J_1)/2$. The exchange energy per unit cell containing four Mn atoms is proportional to $4J_{\rm eff}$.

The field induced changes in the Mn_2Au magnetic moment arrangement were analyzed with the help of the energy density functional, where ϵ is the energy per unit cell volume ($V_{u.c.}$) [Fig. 4]. It includes exchange and Zeeman energy, magneto-crystalline anisotropy energy (MAE) and shape anisotropy:

$$\epsilon = \epsilon_{\rm exchange} + \epsilon_{\rm MAE} + \epsilon_{\rm shape} + \epsilon_{\rm Zeeman}. \tag{3}$$

In the following, the tilting angle (α) of the Mn spins towards the film normal is assumed

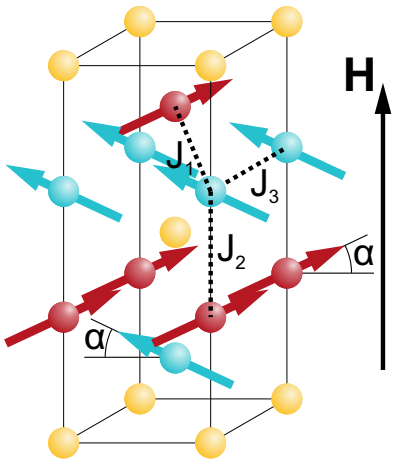

FIG. 4. The elementary cell of Mn_2Au, with Mn atoms drawn in blue and Au atoms in red, featuring the Mn spins reoriented in magnetic field applied along [001] direction. Three different exchange constants are specified following the notations from [16].

to be small [see Fig. 4]. The exchange energy is given by:

$$\epsilon_{\text{exchange}} = -4J_{\text{eff}}\,\cos(\pi - 2\alpha) \sim 8J_{\text{eff}}\,\alpha^2, \tag{4}$$

where the constant term defining the zero-energy value is omitted. The dominant out-of-plane term in the MAE results in:

$$\epsilon_{\text{MAE}} = 4K_{2\perp}\,\sin^2\alpha \sim 2K_{2\perp}\,\alpha^2, \tag{5}$$

where $K_{2\perp}$ is the Mn_2Au anisotropy coefficient equal to 2.44 meV/f.u. [21]. The shape anisotropy appears due to the induced perpendicular magnetization in the film $M_S \sin\alpha$, which creates a demagnetizing field of $\mu_0 M_{\text{S}} \sin\alpha$. The corresponding energy density reads [22]:

$$\epsilon_{\text{shape}} = \frac{\mu_0 M_{\text{S}}^2}{2}\,V_{\text{u.c.}}\,\sin^2\alpha \sim \frac{\mu_0 M_{\text{S}}^2}{2} V_{\text{u.c.}}\,\alpha^2, \tag{6}$$

where M_{S} is the Mn_2Au saturation magnetization and $V_{\text{u.c.}}$ is the unit cell volume.

The resulting total energy is written as:

$$\epsilon = (8J_{\text{eff}} + 2K_{2\perp} + \frac{\mu_0 M_{\text{S}}^2}{2}\,V_{u.c.})\left(\frac{\mu_{\text{S}}}{\mu_{\text{S}}^{\text{Mn}}}\right)^2 - 4(\mu_{\text{S}} + \mu_{\text{L}})\mu_0 H, \tag{7}$$

where α is replaced by $\mu_{\text{S}}/\mu_{\text{S}}^{\text{Mn}}$.

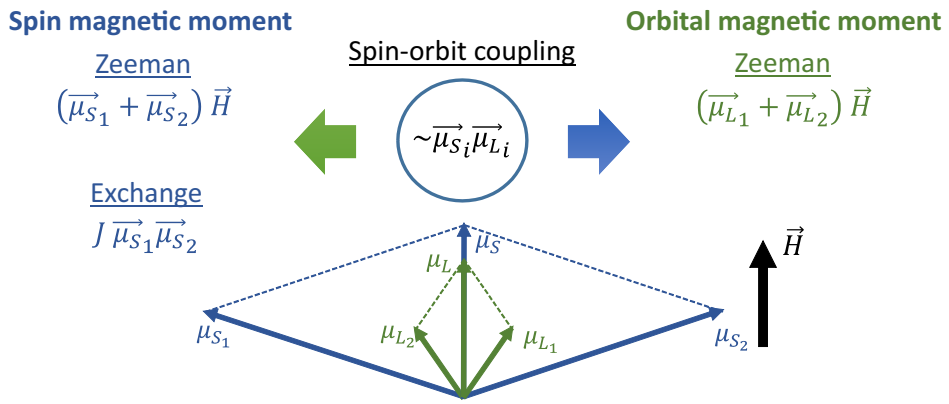

FIG. 5. The spin (μ_{S_1} and μ_{S_2}) and the orbital (μ_{L_1} and μ_{L_2}) magnetic moments of two Mn_2Au sublattices in external magnetic field. Spin-orbit coupling couples the spin and the orbital moment of the same sublattice.

Note that both types of AF domains in a Mn_2Au (001) film, with the Néel vector pointing along the [110] and along the [1$\bar{1}$0] crystallographic directions [17, 23], produce the same contributions to the induced magnetic moment in an out-of-plane field. Minimizing Eq. (7) with respect to the spin magnetic moment value, the following expression for J_{eff} is obtained:

$$J_{\text{eff}} = \frac{\mu_S^{Mn}}{4}\mu_0 H \frac{\mu_S^{\text{Mn}}}{\mu_S} - \left(\frac{K_{2\perp}}{2} + \frac{\mu_0 M_S^2}{8} V_{\text{u.c.}}\right). \tag{8}$$

Inserting values in Eq. (8) from our experiments at 300 K we find for $J_{\text{eff}} = (22 \pm 5)$ meV. It is worth mentioning that the last two terms in Eq. (8) amount to a few percent of the total value. This indicates that the response of the AFM coupled spins to an external field is mainly defined by the exchange interaction. The obtained J_{eff} is considerably smaller than the theoretically predicted value of 90 meV from Ref. [16] and the experimentally determined value of 75 meV reported earlier [9]. The reason for this discrepancy can be the reduction of the exchange constant value in the near-interface region of a thin film or the presence of loose spin clusters contributing to the susceptibility even at room temperature.

b. Perpendicular orbital magnetic moment

The large measured values of μ_L can be interpreted with the following simple model [Fig. 5]. The spin magnetic moments of both sublattices are strongly coupled antiparallel to each other via exchange interaction, which the magnetic field counteracts on [left side of Fig. 5]. The orbital magnetic moments are coupled to the spin moments via spin-orbit

coupling [central part of the Fig. 5]. This model requires a sizable (not fully quenched) orbital moment of the magnetic atoms. The spin-orbit interaction constant is one order of magnitude smaller than the exchange energy [24]. Therefore, the external field rotates the orbital magnetic moments by a larger angle out of their equilibrium position than the spin moments. A similar non-collinear arrangement of spin and orbital magnetic moment has also been found in ferromagnets [24]. As a result, the projected perpendicular orbital moment is of the same magnitude as the projected spin moment. Hence, the non-collinear arrangement of spin and orbital moment explains the observed large orbital to spin moment ratio. Our experimental results strongly suggest that the exchange interaction couples only the spin moments and not the orbital moments. Thus, the perpendicular field causes a larger tilt angle of the orbital moments than of the spin moments.

c. Perpendicular susceptibility of loose spins

The loose spins lead to an increase of the magnetic susceptibility at low temperatures. The induced perpendicular moment of antiferromagnetically coupled atoms is independent of temperature well below T_N. Thus, the room temperature value determined at 8 T can be extrapolated to lower magnetic fields and subtracted from the measured total moment at low temperature to find the loose spin contribution [Fig. 6(a)].

For further analysis, the induced moment of the loose spins is expressed in terms of magnetization using the Mn atom density of $4.2 \times 10^{28}\,\mathrm{m}^{-3}$. The Brillouin function fit [Eq. (1)] to the field dependent induced magnetization of the loose spins is presented in figure 6(b). The saturation magnetization M_S^{loose} of the loose spins is a fitting parameter with the best fit value of $M_S^{loose} = 86\,\mathrm{kJ\,T^{-1}\,m^{-3}}$. This value corresponds to a number of loose spins per volume of $2.6 \times 10^{26}\,\mathrm{m}^{-3}$ or 6 % of all Mn spins in the $\sim$3 nm near-surface layer probed by x-ray absorption. This seems to be a reasonable value considering the determined grain size and the material stoichiometry (see Section II) with additional inter-site disorder.

VI. CONCLUSIONS

Using XMCD, the perpendicular susceptibility of a 10 nm thick Mn_2Au layer in a high magnetic field has been determined. From the perpendicular susceptibility, we find an effec-

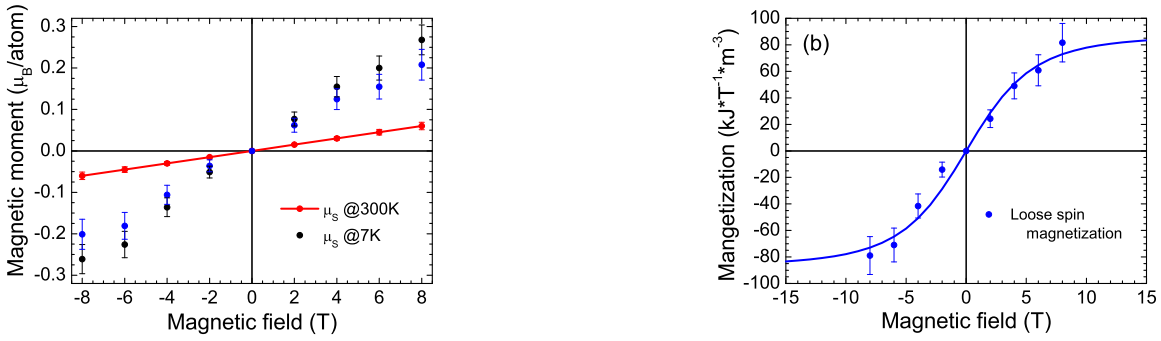

FIG. 6. (a) Field dependence of the spin magnetic moment at 7 K and extrapolated values at 300 K. The difference yields the contribution of loose spins at a temperature of 7 K and assuming that their moments are equally distributed over all Mn atoms. (b) The magnetization of loose spins follows the Brillouin function providing the best fit to the experimental data with a saturation magnetization of 86 kJ T^{-1} m^{-3}.

tive exchange constant of (22 ± 5) meV. The measured orbital magnetic moment is surprisingly large and amounts to about 30 % of the spin moment. A model considering exclusively spin-spin exchange coupling in combination with a weaker spin-orbit coupling is proposed for explaining this phenomenon. Complementary measurements at low temperatures provided the concentration of loose spins in the near-surface region, which for our sample turns out to be 6 % of the total amount of Mn spins in Mn_2Au. The presented procedures for determining effective exchange constants, magnetic moments, and loose spin concentrations via XMCD measurements can be used for characterizing a wide range of AF materials, which is important for identifying novel materials suitable for AF spintronics applications.

The research was financially supported by the German Research Foundation (Deutsche Forschungsgemeinschaft) through the Transregional Collaborative Research Center 173 "Spin+X", Project A05. A. A. S. also wishes to acknowledge the fellowship of the MAINZ Graduate School of Excellence. We thankfully acknowledge the financial support from HZB. The authors also gratefully acknowledge the computing time granted on the supercomputer Mogon at Johannes Gutenberg University Mainz (hpc.uni-mainz.de). Financial support for developing and building the PM2-VEKMAG beamline and VEKMAG end station was provided by HZB and BMBF (05K10PC2, 05K10WR1, 05K10KE1), respectively. Steffen Rudorff is acknowledged for technical support.

[1] V. Baltz, A. Manchon, M. Tsoi, T. Moriyama, T. Ono, and Y. Tserkovnyak, Rev. Mod. Phys. **90**, 015005 (2018).

[2] A. V. Kimel, A. Kirilyuk, A. Tsvetkov, R. V. Pisarev, and Th.. Rasing, Nature (London) **429**, 850 (2004).

[3] T. Kampfrath, A. Sell, G. Klatt, A. Pashkin, S. Mährlein, T. Dekorsy, M. Wolf, M. Fiebig, A. Leitenstorfer, and R. Huber, Nat. Photonics **5**, 31 (2010).

[4] D. Bossini, S. Dal Conte, Y. Hashimoto, A. Secchi, R. V. Pisarev, Th.. Rasing, G. Cerullo, and A. V. Kimel, Nat. Commun. **7**, 10645 (2016).

[5] P. Bowlan, S. A. Trugman, X. Wang, Y. M. Dai, S.-W. Cheong, E. D. Bauer, A. J. Taylor, D. A. Yarotski, and R. P. Prasankumar, Phys. Rev. B **94**, 184429 (2016).

[6] J. Nogués and I. K. Schuller, J. Magn. Magn. Mater. **192**, 203 (1999).

[7] P. Wadley, B. Howells, J. Železný, C. Andrews, V. Hills, R. P. Campion, V. Novák, K. Olejník, F. Maccherozzi, S. S. Dhesi, S. Y. Martin, T. Wagner, J. Wunderlich, F. Freimuth, Y. Mokrousov, J. Kuneš, J. S. Chauhan, M. J. Grzybowski, A. W. Rushforth, K. W. Edmonds, B. L. Gallagher, and T. Jungwirth, Science **351**, 587 (2015).

[8] S. Yu. Bodnar, L. Šmejkal, I. Turek, T. Jungwirth, O. Gomonay, J. Sinova, A. A. Sapozhnik, H.-J. Elmers, M. Kläui, and M. Jourdan, Nat. Commun. **9**, 348 (2018).

[9] V. M. T. S. Barthem, C. V. Colin, H. Mayaffre, M.-H. Julien, and D. Givord, Nat. Commun. **4**, 2892 (2013).

[10] M. Getzlaff, *Fundamentals of Magnetism* (Springer, 2008).

[11] B. T. Thole, P. Carra, F. Sette, and G. van der Laan, Phys. Rev. Lett. **68**, 1943 (1992).

[12] P. Carra, B. T. Thole, M. Altarelli, and X. Wang, Phys. Rev. Lett. **70**, 694 (1993).

[13] M. Jourdan, H. Bräuning, A. Sapozhnik, H.-J. Elmers, H. Zabel, and M. Kläui, J. Phys. D: Appl. Phys. **48**, 385001 (2015).

[14] T. Noll and F. Radu, Proceedings of MEDSI2016 , 370 (2016).

[15] `http://elk.sourceforge.net`.

[16] S. Khmelevskyi and P. Mohn, Appl. Phys. Lett. **93**, 162503 (2008).

[17] V. M. T. S. Barthem, C. V. Colin, R. Haettel, D. Dufeu, and D. Givord, J. Magn. Magn. Mater. **406**, 289 (2016).

[18] I. Galanakis, Phys. Rev. B **71**, 012413 (2005).

[19] E. Goering, Philos. Mag. **85**, 2895 (2005).

[20] A. Scherz, H. Wende, C. Sorg, C. Baberschke, J. Minár, D. Benea, and H. Ebert, Phys. Scr. **T115**, 586 (2005).

[21] A. B. Shick, S. Khmelevskyi, O. N. Mryasov, J. Wunderlich, and T. Jungwirth, Phys. Rev. B **81**, 212409 (2010).

[22] A. Aharoni, *Introduction to the theory of ferromagnetism* (Oxford university press, 2007).

[23] A. A. Sapozhnik, R. Abrudan, Y. Skourski, M. Jourdan, H. Zabel, M. Kläui, and H.-J. Elmers, Phys. Stat. Solidi (RRL) **11**, 1600438 (2017).

[24] H. A. Dürr, G. Y. Guo, G. van der Laan, J. Lee, G. Lauhoff, and J. A. C. Bland, Science **277**, 213 (1997).